Thermochimica Acta, 213 (1993) 151–164
Elsevier Science Publishers B.V., Amsterdam

Thermal characteristics of poly-BAMO and poly-BAMO/BDNPA/BDNPF blends

Shin-Ming Shen, Yih-Shun Chiu and Sun-I Chen

The Fourth Division, Chung Shan Institute of Science and Technology, Lung-tan (Taiwan)

(Received 9 April 1992)

Abstract

The thermal behaviors of polymer blends, mixtures of cured poly-BAMO (mol. wt. = 2000) and eutectic mixtures of bis-2,2-dinitrosopropyl acetal (BDNPA) and bis-2,2-dinitropropyl formal (BDNPF), were examined by thermogravimetry, differential thermogravimetry, differential scanning calorimetry and dynamic exothermic reaction testing. The thermal decomposition reaction of a poly-BAMO/BDNPA/F blend at a dynamic heating rate is indicated by three major stages of weight loss in the TG–DTG traces. The DSC trace indicates that two exothermic reactions exist for each formulation. It was found that the decomposition temperatures of poly-BAMO/BDNPA/F blends were shifted to lower temperatures as ferruginous catalyzer was added.

INTRODUCTION

In order to increase the energy content of composite propellants and plastic bonded explosives, more knowledge is needed concerning the thermal behaviors of the energetic ingredients, such as the binder, oxidizer, plasticizer and the composites composed of these [1–9]. The application of thermo-analytical techniques such as differential thermal analysis (DTA), thermogravimetry (TG), differential scanning calorimetry (DSC), to explosives and propellant ingredients is well established. Each individual technique has inherent value, but a combination of two or more has proved to be invaluable for the study of explosives, propellants and other composite systems [10–17].

The object of this study is to investigate the thermal behaviors of the energetic binder systems of poly-bisazidomethyl oxetane (poly-BAMO), poly-BAMO/BDNPA/F, and the poly-BAMO/BDNPA/BDNPF/ferruginous catalyzer system. All the systems were examined by TG–DTG and DSC. In addition, vacuum stability tests and dynamic exothermic

Correspondence to: Shin-Ming Shen, The Fourth Division, Chung Shan Institute of Science and Technology, Lung-tan, Taiwan.

deflagration temperature tests were carried out to provide a comparison with the DSC results.

EXPERIMENTAL

Materials

The poly-BAMO prepolymer and the nitroplasticizer BDNPA/BDNPF examined in this study were laboratory-synthesized. All the ferruginous catalyzers were obtained from Aldrich. The crosslinking agent N-100 is a commercially available triisocyanate. The general specification of the nitroplasticizers BDNPA, BDNPF and BAMO are listed in Table 1.

TABLE 1

Physical properties of BDNPA, BDNPF, BDNPA/F and poly-BAMO

Compound [a]	Boiling point (°C)	Melting point (°C)	Density at 25°C ($g\ ml^{-1}$)
BDNPA	150	33–34	1.366
BDNPF	152	31	1.411
BDNPA/F	150	−15	1.383
Poly-BAMO	–	≈62	1.3

[a] Molecular formulas:

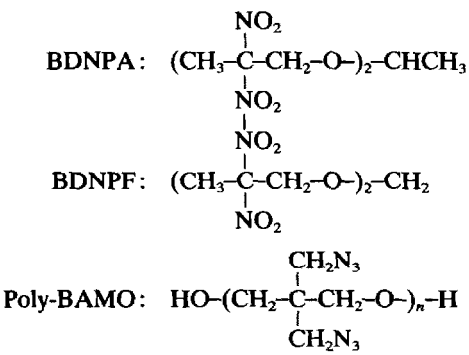

Sample preparation

The polymer blends were generally formulated to an NCO/OH ratio of 1:1. All the polymer blends were prepared by a one-step method. The ingredients were dried to a moisture content of less than 0.02%. The compositions of each sample are listed in Table 2. The mixture of

TABLE 2

Compositions and weight-loss ratios at various TG–DTA measurement stages

Sample	Composition (wt.%) [b]					Weight-loss ratio (wt.%)		
	BAMQ	BDNPA/F	I	II	III	1st stage	2nd stage	3rd stage
A_1 [a]	100	–	–	–	–	38	39.2	–
A_2 [a]	100	–	–	–	–	40.6	36.4	–
B	75	25	–	–	–	27	29.2	23.5
C	50	50	–	–	–	55.5	16	16
D	30	70	–	–	–	81.2	11	–
E	27	66	7	–	–	73.7	21.3	–
F	27	66	–	7	–	79.8	19.2	–
G	27	66	–	–	7	78.3	10.7	–

[a] A_1: BAMO test sample not subjected to the vacuum stability test. A_2: BAMO test sample subjected to vacuum stability test.
[b] I, *n*-butyl ferrocene; II, catocene; III, Fe_2O_3.

poly-BAMO prepolymer, crosslinking agent N-100, BDNPA/F and ferruginous catalyzer were cured in an oven at 65°C for 7 days.

TG–DTG measurements

TG–DTG measurements were carried out using a Perkin-Elmer thermal analyzer. In the TG–DTG measurements, test samples weighing

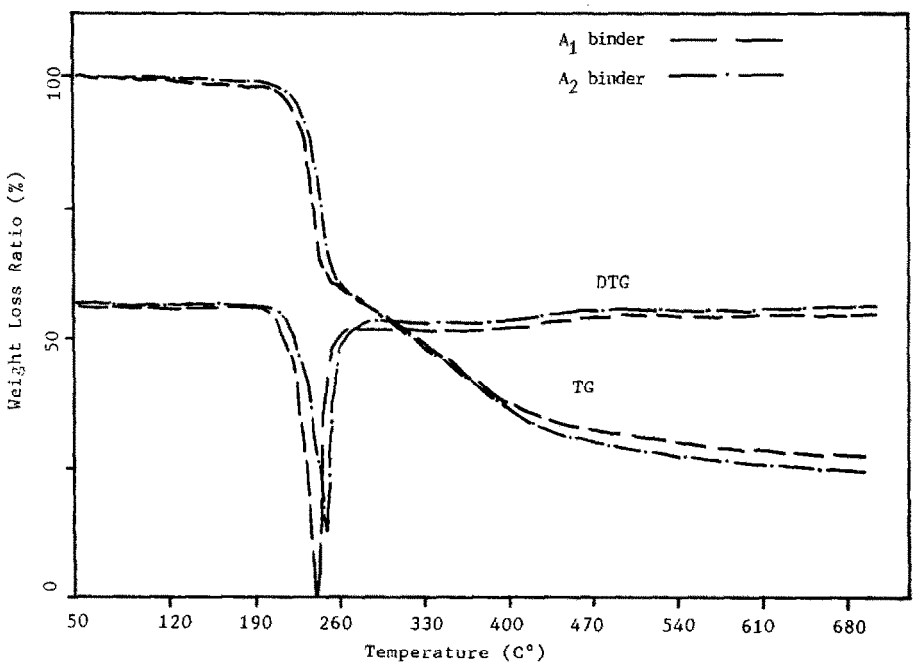

Fig. 1. TG–DTG results for A_1 and A_2 binder.

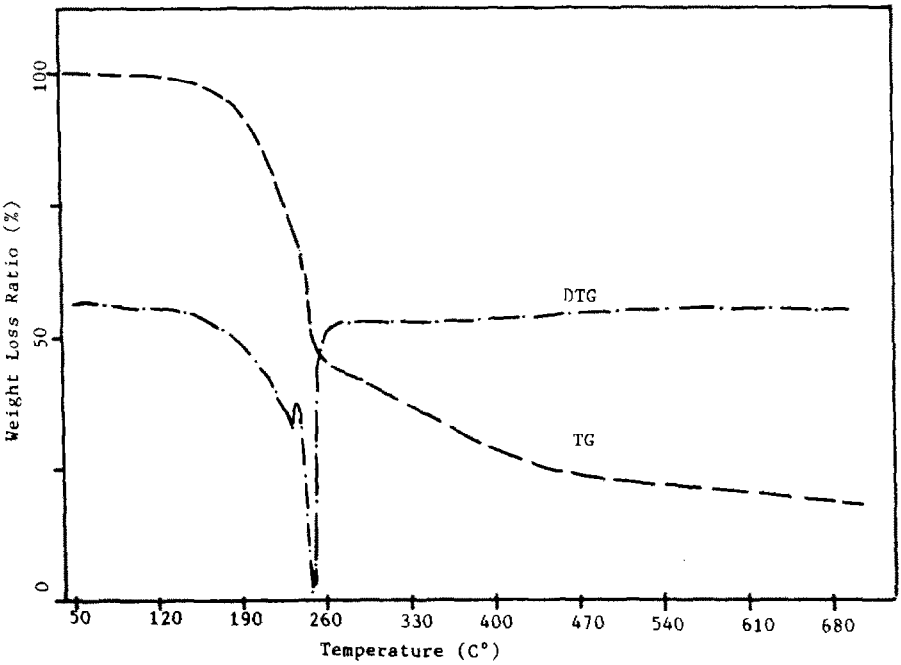

Fig. 2. TG–DTG results for B binder.

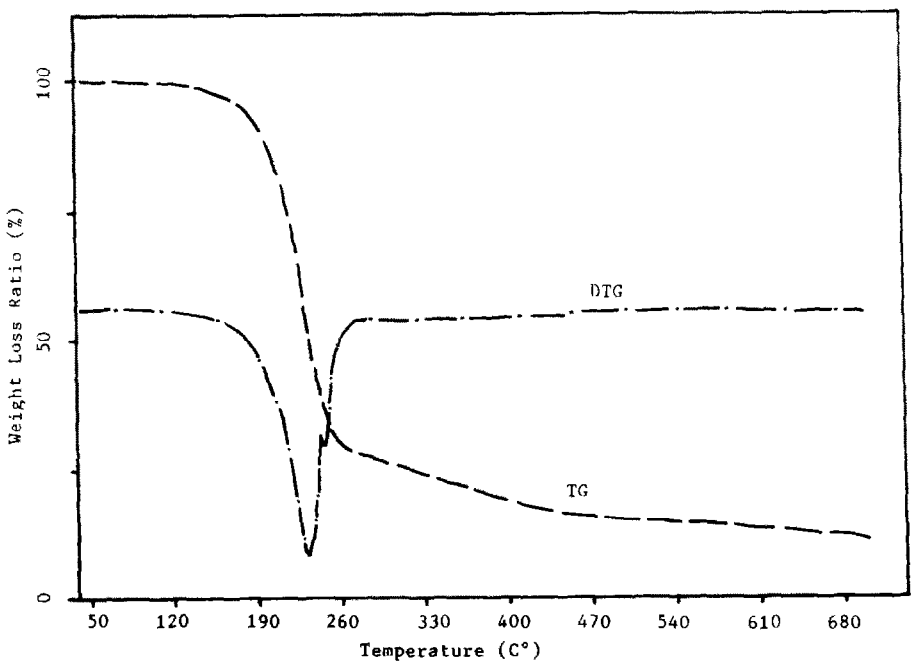

Fig. 3. TG–DTG results for C binder.

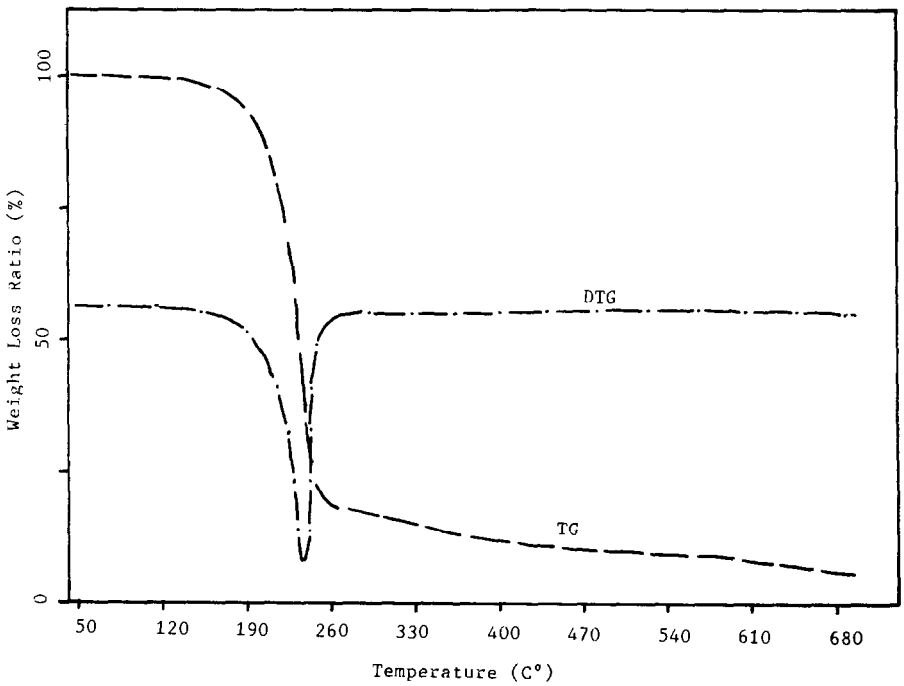

Fig. 4. TG–DTG results for D binder.

3–4 mg were heated at a rate of 5°C min^{-1} from 30 to 500°C under a static atmosphere of nitrogen. The results of the TG–DTG measurement are shown in Figs. 1–4 and in Table 2.

DSC measurements

DSC measurements were performed using Perkin-Elmer and Setaram thermal analyzers. In the DSC measurements, samples weighing 1–2 mg were heated at a rate of 10°C min^{-1} in an aluminum crucible from 30°C to 500°C under a static atmosphere of nitrogen. The results of the DSC measurements are shown in Table 3 and Figs. 5 and 6.

Vacuum stability test

The vacuum stability test was designed to determine the stability of explosives and propellants under vacuum conditions. This test can be made at 100°C, 120°C, or any other desired temperature; a temperature of 100 or 120°C is generally employed. The test sample is placed in a heat tube, heated and the gas liberated measured. In our test, each sample weighing 50 mg was heated for 40 h under vacuum at 100°C. The results are shown in Table 4.

TABLE 3

Maximum reaction temperature (T_m), onset temperature (T_o) and enthalpy change (ΔH) for DSC measurement

Sample	Composition (wt. %) [b]					DSC (heating rate 10°C min^{-1})		
	BAMO	BDNPA/F	I	II	III	T_o (°C)	T_m (°C)	$-\Delta H$ (J g^{-1})
A_1 [a]	100	–	–	–	–	199.6	254.6	2648.5
A_2 [a]	100	–	–	–	–	200.8	249	2682
B	75	25	–	–	–	201	244.6	2493.6
C	50	50	–	–	–	197.8	244.5	2222
D	30	70	–	–	–	197.3	249	1929.7
E	27	66	7	–	–	214.7	217.6	1379.7
F	27	66	–	7	–	190.2	192.5	1608
G	27	66	–	–	7	226.8	229.7	1209.7

[a] A_1: poly-BAMO test sample not subjected to the vacuum stability test. A_2: poly-BAMO test sample subjected to the vacuum stability test.
[b] I, *n*-butyl ferrocene; II, catocene; III, Fe_2O_3.

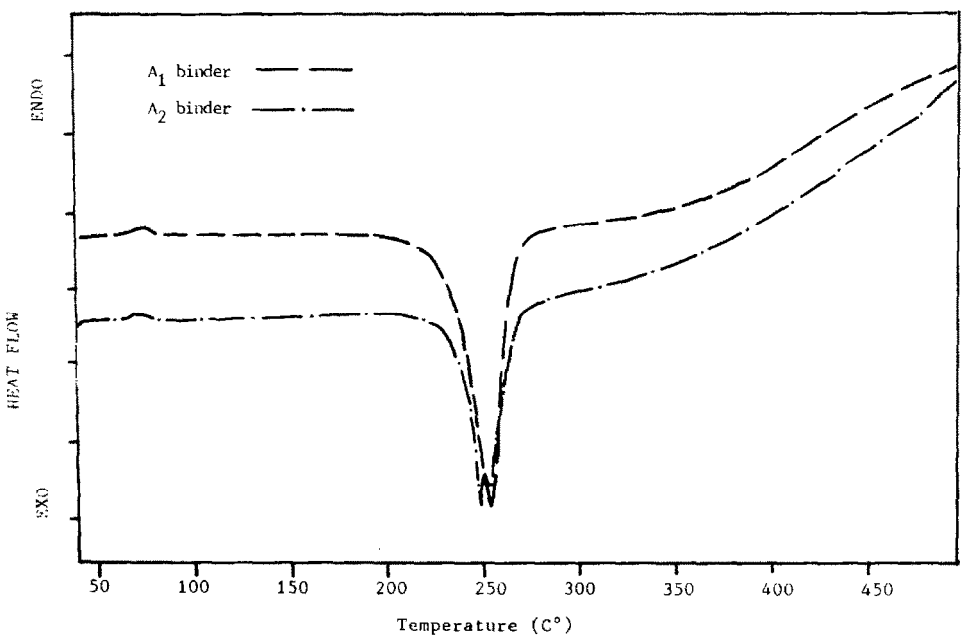

Fig. 5. DSC results for A_1 and A_2 binders.

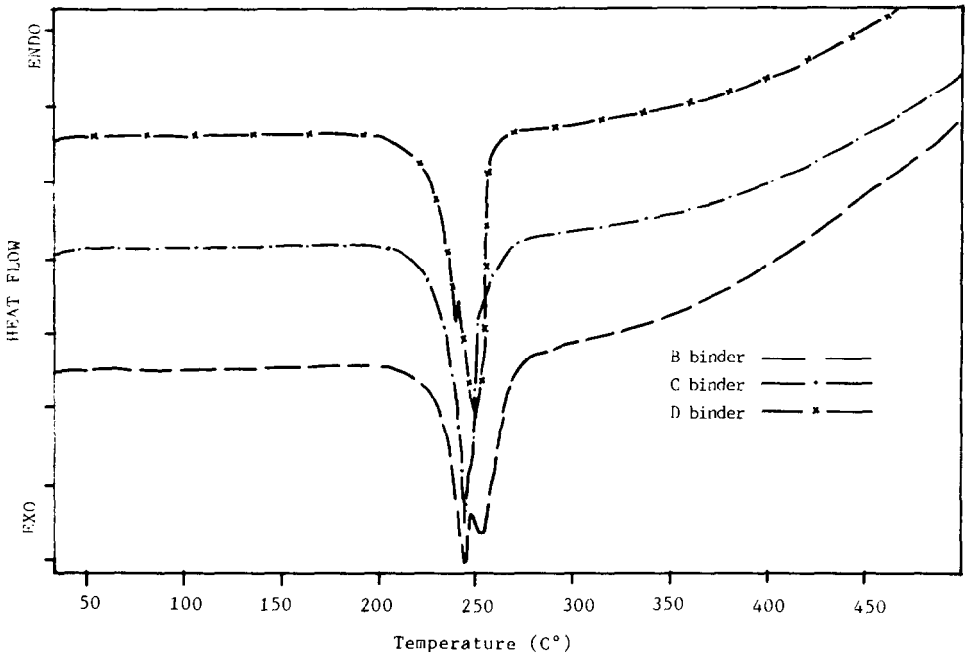

Fig. 6. DSC results for B, C and D binders.

TABLE 4

Vacuum stability and dynamic exothermic test of poly-BAMO and GAP binder systems

Sample	Composition (wt. %) [c]						Vacuum stability test ($ml\ g^{-1}$)	Dynamic exothermic test (°C)
	BAMO	BDNPA/F	GAP	I	II	III		
A_3 [a]	100	–	–	–	–	–	1.304	240
A_4 [b]	100	–	–	–	–	–	–	222
A_5 [a]	–	–	100	–	–	–	0.968	239
A_6 [b]	–	–	100	–	–	–	–	219
B	75	25	–	–	–	–	2.237	222
C	–	25	75	–	–	–	1.452	221
E	27	66	–	7	–	–	1.54	188
F	27	66	–	–	7	–	11.25	186
G	27	66	–	–	–	7	2.17	208

[a] Polymer (uncured).

[b] Polymer (cured).

[c] I, *n*-butyl ferrocene; II, catocene; III, Fe_2O_3.

Dynamic exothermicity test

The apparatus for carrying out the dynamic exothermicity test is shown in Fig. 7. It is a modification of a Woods metal bath with automatic temperature recording. Three specimens are placed in a round block of high heat-conducting brass dipped in Woods metal melt, using electrical heating, which is installed in a casing of steel sheeting. Automatic regulation of the increase in temperature for the test sample was made by means of a contact thermometer for the rate of increase desired. In this study the minimum temperature at which a substance can undergo exothermic decomposition is estimated. The test sample weighed about 300 mg. The temperature difference between test sample and heater was recorded, and the results are shown in Figs. 8–11 and listed in Table 4.

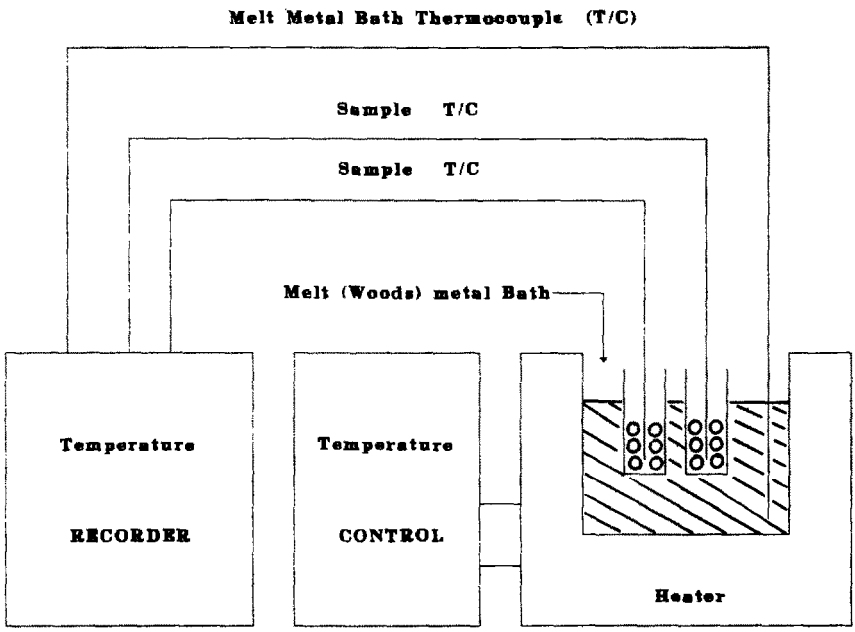

Fig. 7. Apparatus for the dynamic exothermicity test.

RESULTS AND DISCUSSION

Figures 1–4 show the TG–DTG traces for each system. In the TG–DTG measurement, it was found that two weight-loss reactions take place for the A_1 and A_2 (pure) BAMO binder systems. Table 2 shows the

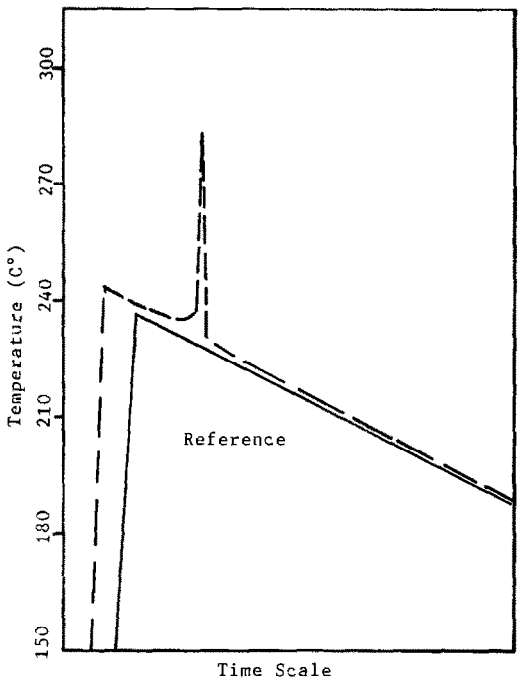

Fig. 8. Dynamic exothermicity test result for A_1 binder.

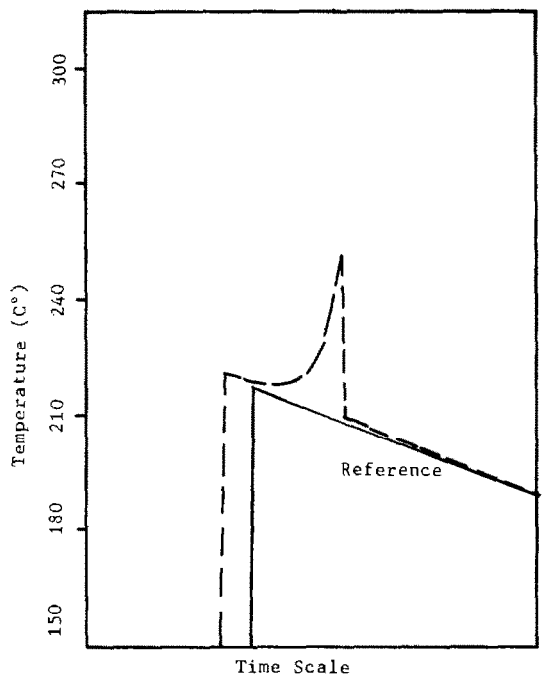

Fig. 9. Dynamic exothermicity test result for E binder.

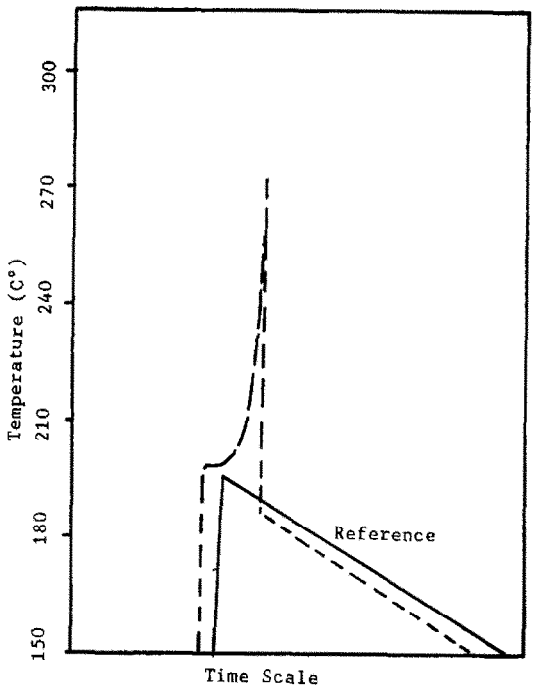

Fig. 10. Dynamic exothermicity test result for F binder.

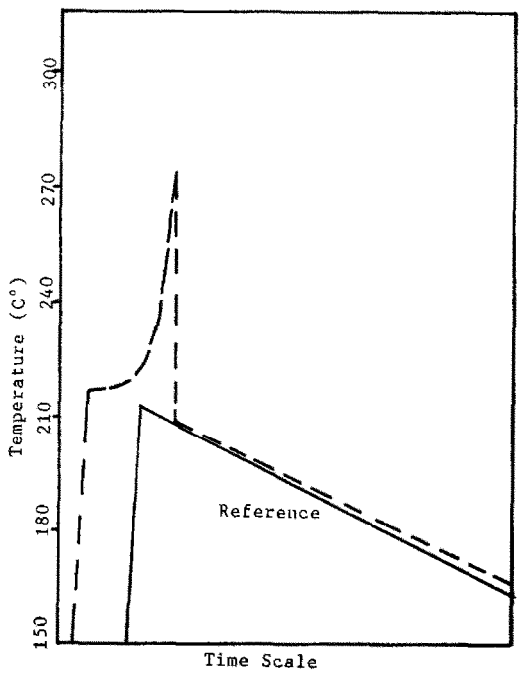

Fig. 11. Dynamic exothermicity test result for G binder.

weight loss ratios of each test sample. Formulation A_1 is poly-BAMO binder which has not been vacuum-stability tested and formulation A_2 is poly-BAMO binder which has been vacuum-stability tested. It was found that the weight loss ratios of the A_1 and A_2 systems are not remarkably different from each other. Figure 5 shows the DSC patterns of formulation A_1 and formulation A_2. There is one exothermic reaction peak for the formulation A_1 system, but for formulation A_2 there is an overlapping exothermic reaction peak. The ΔH values of A_1 and A_2 are 2648 and 2682 J g^{-1}, respectively.

From the DSC and TG–DTG measurement results, it is shown that there are two weight-loss stages for the poly-BAMO binder itself. The first stage corresponds to an exothermic reaction. During the second stage, a slow weight-loss reaction occurred without heat release. These results are similar to those for the GAP binder systems whose thermal decomposition behaviors have been reported previously [6, 8].

FTIR patterns of the A_1 and A_2 formulations are shown in Figs. 12 and 13, respectively. It is shown that the poly-BAMO structure undergoes no remarkable change after a vacuum stability test. Therefore, a further investigation into the variation of the poly-BAMO decomposition mechanism is required. Formulations B, C, and D are BAMO binder which various weight ratios of BDNPA/F plasticizer. In the TG–DTG measure-

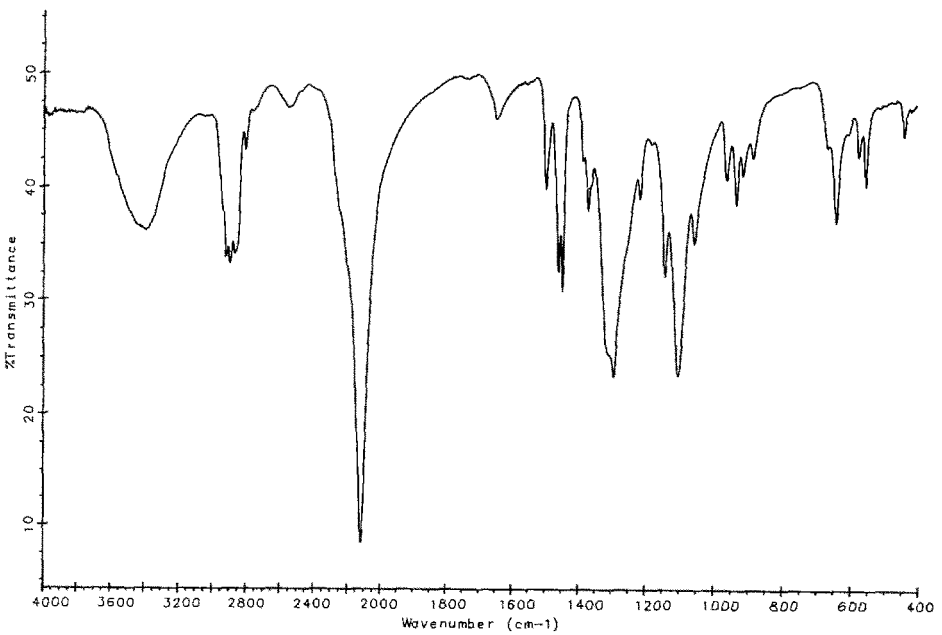

Fig. 12. FTIR pattern for A_1 binder.

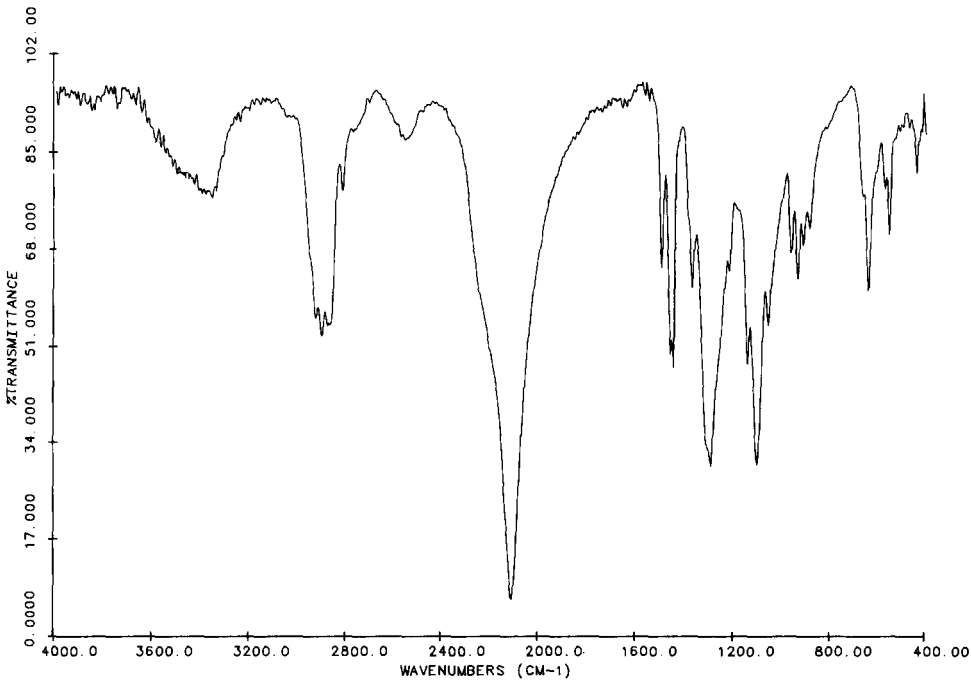

Fig. 13. FTIR pattern for A_2 binder.

ment of formulation B (25% BDNPA/F), there are three weight-loss reactions, the weight-loss ratios being 27%, 29% and 24% at 231, 247 and 260–500°C, respectively. For formulation C (50% BDNPA/F), there are also three weight-loss reactions, the weight-loss ratios being 55.5%, 16% and 16% at 233, 248 and 260–500°C, respectively. For the D system, the weight-loss ratios are 81.2% and 11% at 235 and 266–500°C, respectively.

The DSC patterns of formulations B, C, and D are shown in Fig. 6 which shows an overlapping exothermic peak for formulations B, C and D. For the BAMO/BDNPA/F systems, a three-stage weight-loss process was found. Comparing the weight-loss ratios with the percentage of ingredients for each formulation and the combined DSC and TG–DTG results, shows that BDNPA/F decomposed before BAMO. There is an overlapping reaction peak due to the close decomposition reaction temperatures (T_0) of BDNPA/F (220°C) and poly-BAMO (232°C). These decomposition behaviors are similar to the GAP/BDNPA/F system reported earlier [8]. The combined DSC patterns of formulations E, F, and G are shown in Fig. 14. These patterns were recorded on a Setaram TG–DSC 111 thermal analyzer. Table 3 shows the reaction temperature of T_m which shifts to lower temperatures when a ferruginous compound is added to the BAMO/BDNPA/F binder system; this proves that ferruginous compounds can effect the decomposition temperature of BAMO/BDNPA/F binder.

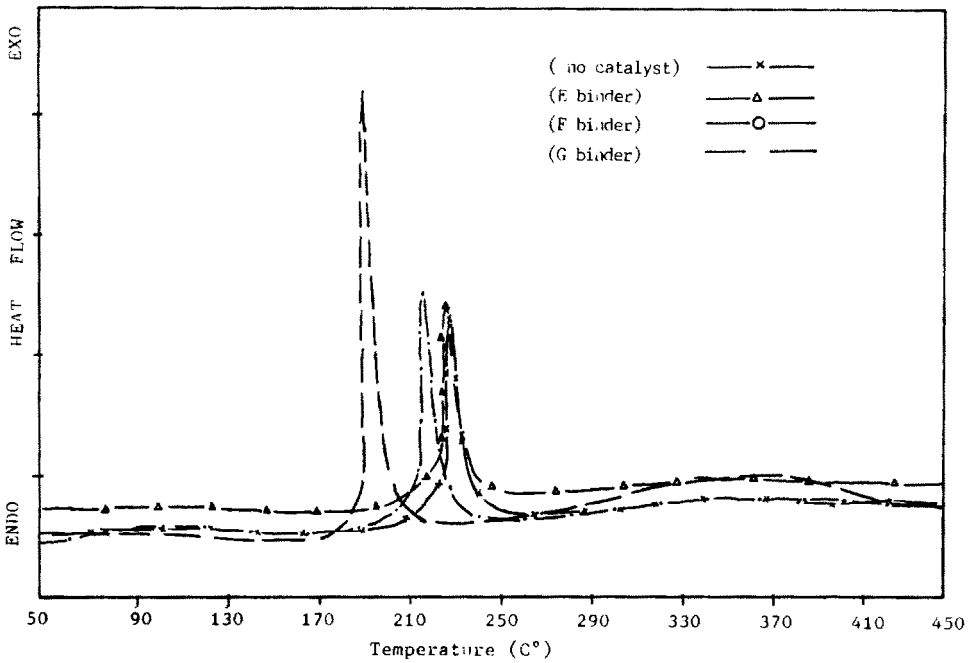

Fig. 14. TG–DSC pattern for E, F and G binder.

In order to confirm the interrelation trend of the T_m observed in the DSC, a comparison was made of the DSC measurement results and the deflagration reaction temperatures T_{dr}, obtained by the dynamic exothermicity test. The reaction curves and T_{dr} values obtained from the dynamic exothermicity tests for each formulation are shown in Figs. 8–11 and Table 4. From the dynamic exothermicity test, which was carried out using large sample masses, the changing trend of reaction temperatures of E, F and G were obtained: they are similar to the DSC test results shown in Tables 3 and 4. Comparing the values of T_m from DSC and T_{dr} from dynamic exothermicity testing, it was shown that the T_{dr} reaction temperatures are lower than the T_m for each system. The sample mass employed for the dynamic exothermicity test is one hundred times that of the DSC measurement. The decomposition conditions of samples of high mass are more similar to those used in practice. Therefore, the results from the dynamic exothermicity data are more useful or energetic materials.

It is also noted that the use of catocene caused more gases to be liberated in the vacuum stability tests than occurred with the other ferruginous catalysts. Ferruginous materials are used as burning-rate modifiers for most composite propellant systems and further investigation of the reaction mechanism is suggested.

CONCLUSION

The thermal decomposition of cured BAMO and BDNPA/F blends indicates a two-stage reaction. The first stage corresponds to the

BDNPA/F decomposition, and the second stage corresponds to the decomposition of BAMO molecules. The FTIR patterns indicate that the structure of the BAMO binder is unchanged after the vacuum stability test. The addition of a ferruginous compound decreases the decomposition temperature of the BAMO/BDNPA/F binder system.

REFERENCES

1 A.M. Helmy, 20th Joint Propulsion Conf., 11–13 June 1984, Cincinnati, OH, American Institute of Aerospace and Astronautics, paper no. 84-1434, 1984.
2 K. Klager, 20th Joint Propulsion Conf., 11–13 June 1984, Cincinnati, OH, American Institute of Aerospace and Astronautics, paper no. 84-1239, 1984.
3 A.M. Helmy, 23rd Joint Propulsion Conf., 29 June–2 July 1987, San Diego, CA, American Institute of Aerospace and Astronautics, paper no. 87-1725, 1987.
4 S.Y. Ho and C.W. Fong, J. Mater. Sci., 22 (1987) 3023.
5 A. Chin, D. Rankin and B.R. Hubble, Insensitive pyrotechnics—improved binders for colored smokes, Proc. 13th Int. Pyrotechnic Seminar, Grand Junction, USA, July 1988, pp. 129–134.
6 N. Kubota and T. Sonobe, Propellants, Explosives, Pyrotechnics, 13 (1988) 172.
7 S.M. Shen, A.L. Leu and H.C. Yeh, Thermochim. Acta, 176 (1991) 75.
8 S.M. Shen, A.L. Leu, S.I. Chen and H.C. Yeh, Thermochim. Acta, 180 (1991) 251.
9 S.M. Shen, F.M. Chang, J.C. Hu and A.L. Leu, Thermochim. Acta, 181 (1991) 277.
10 Z.R. Liu, C.M. Yin, C.Y. Wu and M.N. Chang, Propellants, Explosives, Pyrotechnics, 11 (1986) 10.
11 N.E. Beach and V.K. Canfield, Compatibility of Explosives with Polymer, Picatinny Arsenal, Dover, New Jersey, AD-721004, 1971.
12 L. Reich, Thermochim. Acta, 5 (1973) 433.
13 L. Reich, Thermochim. Acta, 8 (1974) 399.
14 J.H. Bae, J. Therm. Anal., 4 (1972) 261.
15 R.T. Yang, Anal. Chem., 49 (7) (1977) 998.
16 A.S. Tompa, Thermochim. Acta, 63 (1983) 9.
17 J.N. Maycock, Thermochim. Acta, 1 (1970) 387.